IOP Publishing

Journal of Physics D: Applied Physics

J. Phys. D: Appl. Phys. **48** (2015) 235103 (5pp)

doi:10.1088/0022-3727/48/23/235103

Surge current capabilities and isothermal current–voltage characteristics of high-voltage 4H-SiC junction barrier Schottky rectifiers

J W Palmour[1] M E Levinshtein[2], P A Ivanov[2] and Q J Zhang[1]

[1] Cree Inc., 4600 Silicon Dr., Durham, NC 27703, USA
[2] Ioffe Institute, 26 Politekhnicheskaya, 194021 St. Petersburg, Russia

E-mail: melev@nimis.ioffe.ru

Received 26 January 2015, revised 20 April 2015
Accepted for publication 21 April 2015
Published 14 May 2015

Abstract

Isothermal forward current–voltage characteristics of high-voltage 4H-SiC junction barrier Schottky rectifiers (JBS) have been studied for the first time. Isothermal characteristics were measured with JBS having a blocking voltage of 1700 V up to a current density $j \approx 4200\,\mathrm{A\,cm^{-2}}$ in the temperature range 297–460 K. Quasi-isothermal current–voltage characteristics of these devices were studied with injection of minority carriers (holes) up to $j \approx 7200\,\mathrm{A\,cm^{-2}}$ and ambient temperatures of 297 and 460 K. The isothermal forward current–voltage characteristics make it possible to numerically calculate (for example, by an iteration procedure) the overheating in an arbitrary operation mode.

Keywords: silicon carbide, Schottky diodes, forward bias, high current density, minority carriers

(Some figures may appear in colour only in the online journal)

1. Introduction

Schottky barrier diodes (SBDs) are among the most common devices of semiconductor electronics. They are widely used in high-frequency applications as detectors, mixers and non-linear elements up to gigahertz frequencies. Schottky Barrier Diodes are also suitable for the electrostatic discharge (ESD) protection of sensitive devices. Power SBDs are widely used in low voltage switched-mode power supplies in PCs, motor vehicles, and power factor correction systems (PFCs) [1]. The main advantage of SBDs is that their switching speed is very high, and the switching loss is extremely low. These advantages are due to the fact that the Schottky diodes are majority-carrier devices and minority carriers do not accumulate in the base of the device during the forward current flow. However, the positive temperature coefficient of the forward voltage and the lack of conductivity modulation cause a rather large voltage drop across the base of SBDs and thereby limit the ability of Schottky diodes to sustain high surge currents. As a result, SBDs show a poorer working capacity at relatively small current densities in comparison with p-n rectifiers [2–4]. Merged p-i-n/Schottky (MPS) rectifiers or junction barrier Schottky rectifiers (JBS) have been proposed to overcome this difficulty [5].

The JBS is an integrated structure in which the Schottky diode regions are interspersed with local p-n-regions. The p-regions are closely spaced so that the depletion regions of adjacent p-n junctions overlap under a reverse bias. As a result, the leakage currents decrease to the values characteristic of reverse-biased p-n junctions. At a rated forward bias, the forward current flows only through the Schottky contact regions. However, when very high current densities are flowing through the device, the minority carriers are injected from the p-n junctions, which substantially reduce the forward voltage drop across the base (see, for example, [5–10]).

In designing these devices, a compromise is usually sought for between the reverse leakage current, the area occupied by p-n junctions, and the ability to endure surge currents. In JBS intended for use in high-power high-voltage pulse circuits, it is also essential to find the compromise between the ability to endure surge currents and the need to limit the injection from the p-n junction, because the presence of minority carriers drastically diminishes the operation speed of the device.

The temperature of the junction (Schottky barrier or p-n junction) is the critical parameter that predetermines the failure of a device under surge current conditions. The maximum current density at which this critical temperature is reached depends on the operation mode. It is necessary to distinguish between three characteristic current surge modes [11].

The first limiting case of an 'infinitely long' pulse corresponds to the self-heating in the *dc mode*. The overload characteristics of the device in this mode are mainly determined by the substrate thickness, diameter of the diode structure, and thermal characteristics of the heat-sink [12]. The opposite limiting case of a '*short' pulse* corresponds to a very short current pulse width t_0, during which heat does not have enough time to reach the heat sink. The 'industrial standard' for such a pulse is 8/20 μs pulse, i.e. a triangular pulse with 8 μs rise and 20 μs fall time. At the same time, rectangular current pulses with pulse duration $t_0 \approx 20$–$50\,\mu$s are not infrequently used to characterize the ability of the diodes to withstand such short pulse current surge. The intermediate case corresponds to '*long' surge pulse*. This pulse is given as a surge current rating for a 60- or 50 Hz half-cycle sine wave or a 8–10 ms rectangular pulse [3, 13]. In this mode, the heat released in the active region of the diode has enough time to reach the heat-sink.

In the short-pulse mode it is easy to estimate the overheating, ΔT by using a simple approximate formula:

$$\Delta T \approx \frac{A}{C(T)\cdot\rho\cdot[W+L_{\mathrm{T}}(T)]\pi[a/2+L_{\mathrm{T}}(T)]^2} \tag{1}$$

where $A = I \times U_{\mathrm{d}} \times t_0$ is the total energy released in the device, I is the current, and U_{d} is the voltage drop across the device, C is the specific heat, ρ is the density, W is the base width, a is the diameter of the device, and $L_{\mathrm{T}} = \sqrt{\chi t_0}$ is the characteristic length L_{T} of heat diffusion during a pulse of width t_0. Here $\chi = K/\rho C$ is the thermal diffusivity and K is the thermal conductivity. Making such an estimate, we assume that the whole heat energy A is released in the blocking base and spreads to a length L_{T}.

Calculation of the overheating ΔT for two other modes is, generally speaking, a rather complicated problem [12]. However, this problem can be solved numerically (for example, by an iteration procedure) for any pulse waveform and duration, provided that the *isothermal* current–voltage (*I–U*) characteristics are determined in wide temperature range. It is noteworthy that, by contrast, the experimentally measured non-isothermal *I–U* characteristics describe the overheating only in a given mode and can not be used for versatile calculations.

The *I–U* characteristics of 4H-SiC SBDs and JBS have been extensively studied; however, to the best of our knowledge, *isothermal I–U* characteristics of these devices have not been measured so far.

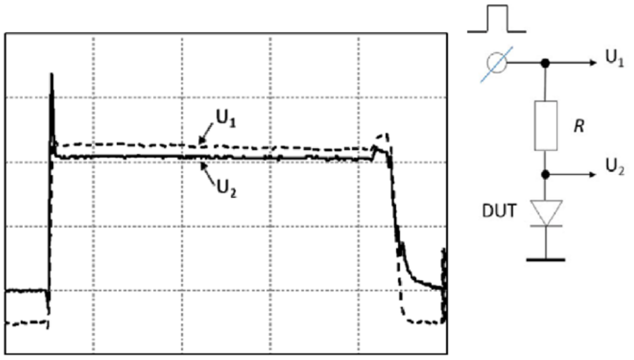

Figure 1. Oscillograms of signals U_1 and U_2 (small biases). U_2 is the forward voltage drop across the device under test (DUT). U_1 is the sum of U_2 and the voltage drop on the series resistor R = 50 Ohm. The horizontal scale is 0.8 μs/div; the vertical scales are 4 V/div (U_1) and 1 V/div (U_2). The inset shows schematically the measuring circuit.

The time dependence of the current was reported in [14] for t_0 = 10 μs and the maximum current density $j_{\max}$ = 4160 A cm^{-2} for a 4H-SiC SBD with a blocking voltage of 600 V. In spite of the relatively small pulse duration, the self-heating was found to be very remarkable. In [15], the pulse duration was 20 ms, i.e. 2000 times that in [13]. Undoubtedly, the *I–U* characteristics of 4H-SiC JBS with a blocking voltage of 1.2 kV, measured in [15] up to $j_{\max} \approx 3000$ A cm^{-2}, can not be considered isothermal. In [16], the current–voltage characteristics of 4H-SiC JBS were measured up to currents that were 10 times the rated currents for the devices. The pulse duration t_0 was in the range 0.5–6 ms. It is clear that, even at the minimum values of t_0, these measurements are far from being isothermal. The *I–U* characteristics of 4H-SiC JBS with a 3.3 kV blocking voltage were measured in [8] up to current densities of 1200 A cm^{-2} in the dc mode.

In this paper, forward *isothermal I–U* characteristics were studied in high-voltage (1700 V) 4H-SiC JBS up to $j \approx 4200$ A cm^{-2}. Quasi-isothermal *I–U* characteristics of these devices were studied, with minority carriers (holes) injected, up to $j \approx 7200$ A cm^{-2} at the ambient temperature of 460 K.

2. Experimental

4H-SiC JBS samples with a working area of the anode contact, $S_{\mathrm{A}} = 5.7 \times 10^{-4}$ cm^2, and the base width $W \approx 18\,\mu$m were fabricated on the basis of commercial CPW3-1700S010 SBDs (1700-V blocking voltage and 10-A forward current) manufactured by Cree, Inc [17]. A photoresist layer with a diameter a = 270 μm was deposited on the anode pad of the commercial structure. After that, the rest of the metallization was removed by etching at room temperature in monoethanolamine-based Al enchant for 1.5 h. Pulsed forward *I–U* characteristics were measured in a nearly current-generator mode. The sample was connected in series with a high-frequency resistor R = 50 Ohm (see inset in figure 1).The pulse rise time was less than 70 ns. The measurements were made in a single-pulse mode. Without the minority carrier injection, the duration of the transient switch-on process was 80 ns (figure 1). In this

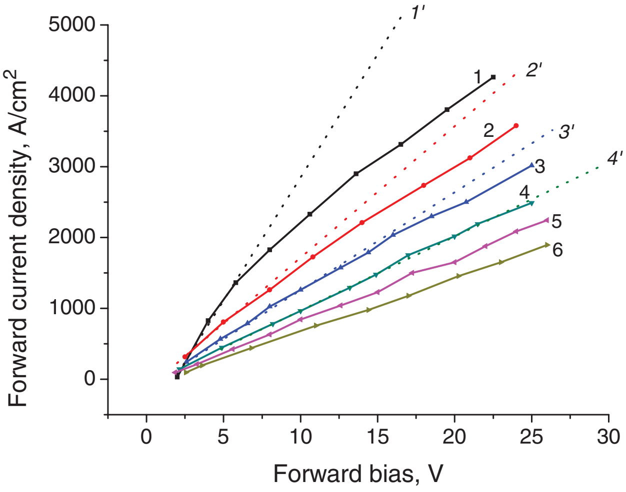

Figure 2. Forward current density versus forward bias for 4H-SiC JBS at different temperatures T (K): 1—297; 2—336; 3—364; 4—398; 5—425; 6—460. The dotted lines 1′–4′ show the slopes of the respective curves 1–4 at a low bias.

case, the voltage and current across the structure were measured 120 ns after the beginning of the pulse.

When minority carriers are injected, the duration of the transient switch-on process substantially increases. The specific features of the measurements in these conditions are discussed below.

3. Results and discussion

Figure 2 shows the isothermal forward current density-forward bias (j-U) characteristics of the samples, measured at different temperatures. No injection was observed up to the maximum values of U, shown in the figure.

It is easy to show that the j-U dependences in figure 2 are isothermal. An estimate of ΔT in accordance with formula (1) gives at room temperature (curve 1 in figure 2), $\Delta T \approx 2$ K at $j = 4200\,\mathrm{A\,cm^{-2}}$, $U = 22.5$ V, $t_0 = 1.2 \times 10^{-7}$ s $W \approx 20\,\mu$m, $\rho = 3.21\,\mathrm{g\,cm^{-3}}$, $C\,(300\,\mathrm{K}) = 0.69\,\mathrm{J\,(g\,K)^{-1}}$, $\chi(300\,\mathrm{K}) = 1.7\,\mathrm{cm^2\,s^{-1}}$ [18]. It is clear from figure 2 that ΔT decreases with increasing temperature, because the value of current density j reduces monotonically with temperature growth at the same value of bias U.

As seen in figure 2, a pronounced tendency to level-off is exhibited by the j-U curves at relatively low temperatures (curves 1–3). The tendency disappears with increasing temperature. This effect can be caused by the saturation of the electron drift velocity, v_d, in strong electric fields. At a doping level $N_d \approx 10^{15}\,\mathrm{cm^{-3}}$, the low-field mobility μ_0 at room temperature may be as high as $800\,\mathrm{cm^2\,(V\,s)^{-1}}$ [19]. At a forward bias $U \approx 22$ V, the voltage drop across the base of the structure is about 20 V, and the average electric field strength $F = U/W \approx 10^4\,\mathrm{V\,cm^{-1}}$. With a linear $v_d(F)$ dependence, $v_d = \mu_0 F \approx 8 \times 10^6\,\mathrm{cm\,s^{-1}}$, i.e. it is more than 1/3 of the maximum saturated value of v_{dmax} in 4H-SiC ($v_{dmax} = v_s \approx 2 \times 10^7\,\mathrm{cm\,s^{-1}}$ [20]). Measurements of $v_d(F)$ dependences in [20] with samples having a noticeably lower mobility $\mu_0 \approx 450\,\mathrm{cm^2V s^{-1}}$ show that, even in samples of this kind, the drift velocity at

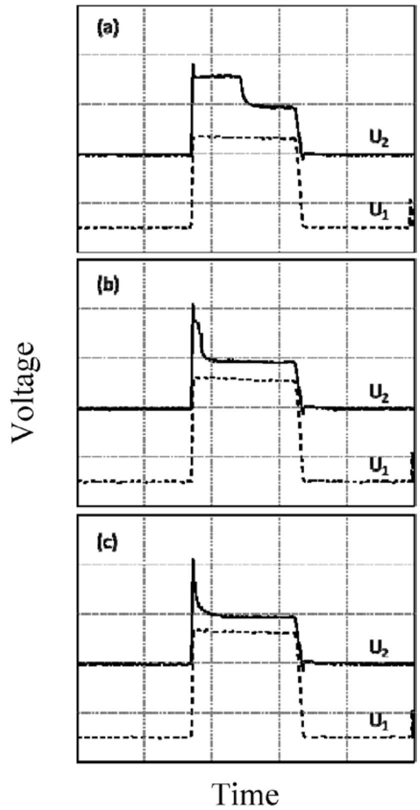

Figure 3. Oscillograms of the forward voltage drop across DUT (U_2) and the sum of U_2 and the voltage drop on the series resistor $R = 50$ Ohm (U_1). High biases. The horizontal scale is 2 μs/div; the vertical scales are 100 V/div (U_1) and 20 V/div (U_2). Steady-state current through the DUT at $t = 3\,\mu$s (A): (a) 3.34, (b) 3.84, (c) 4.04.

$F \approx 10^4\,\mathrm{V\,cm^{-1}}$ is 1.2 times smaller than the value calculated as $v_d = \mu_0 F$. To the best of our knowledge, the $v_d(F)$ dependences have not been measured with high-mobility ($\sim 800\,\mathrm{cm^2\,(V\,s)^{-1}}$) samples so far. Apparently, the electron heating grows with increasing low-field mobility, and the tendency toward saturation of the electron drift velocity must be significantly more noticeable in samples of this kind, compared with samples having lower μ_0. The ratio between the current density estimated from the linear $v_d(F)$ dependence (curve 1′ in figure 2) and its experimental value (curve 1 in figure 2) is ~1.6 at $U = 22$ V. This value of the ratio seems to be quite reasonable.

As expected, the tendency toward saturation of v_d becomes less pronounced with increasing temperature due to the decrease in the low-field mobility. At $T \approx 400$ K (curve 4, figure 2), the tendency toward saturation virtually vanishes.

It is noteworthy that a noticeable injection of holes is observed in the conventional p-n junction at room temperature under a forward bias $U_2 \approx U_{th} \geq 3$–5 V. The value of U_{th} even decreases with increasing temperature [8, 9, 15]. However, it can be seen in figure 2 that hole injection in the samples under study is blocked at $U \leq 25$ V, even at $T = 460$ K.

At $U \geq 25$ V, however, effective hole injection occurs in the whole temperature range 297 K < T < 460 K. In this case, the nature and duration of the transient process changes cardinally. Figure 3 presents examples of the transient process for this case (at room temperature). The nature and duration of

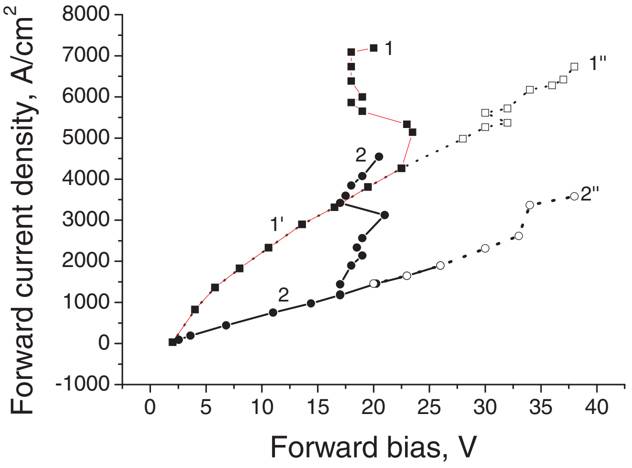

Figure 4. Forward current density versus forward bias for a 4H-SiC JBS, measured in three different modes at two temperatures: (1, 1′, 1″)—297 K; and (2, 2′, 2″)—460 K. Curves 1′ and 2′ coincide with curves 1 and 6 in figure 2. Curves 1″ and 2″ represent the data measured 100 ns after the application of the input pulse. There is no hole injection. Curves 1 and 2 represent the steady-state *j-U* characteristics measured with hole injection 3 μs after the application of the input pulse (see figure 3).

the transient processes at elevated temperatures qualitatively coincide with those at room temperature.

It can be seen in figure 3 that, during a certain time after the beginning of a pulse, the transient processes fully coincide with that in figure 1. However, after a certain interval t_d, the layer blocking the hole injection loses its blocking properties and hole injection occurs. The voltage drop across the sample (U_2) decreases, and the steady-state condition is approached after $t \leq 3\,\mu$s. The general trend traced in figures 3(a)–(c) consists in that the higher the input signal level, the smaller the value of t_d. However, this tendency only occurs 'in general'. The time of beginning of hole injection widely fluctuates from pulse to pulse even at the same level of the input signal (jitter). The situation is reminiscent of so-called 'microplasma breakdown' [21–23].

Figure 4 shows *j-U* characteristics of the JBS under study, measured in three different modes.

It is noteworthy that the dotted curves 1″ and 2″ clearly confirm the absence of injection in the case of very short (≤100 ns) forward bias pulses. For such short pulses the device retains the operating speed characteristic of the Schottky diodes up to forward voltages $U \approx 38$ V. At $U = 38$ V, the heating $\Delta T \approx 5.4$ K at $T = 297$ K and decreases monotonically with increasing temperature. Hence, the current-voltage characteristics represented by curves 1″ and 2″ can also be considered isothermal.

Curves 1 and 2 represent the steady-state *j-U* characteristics in the case of the occurring hole injection. The characteristic time in which the steady-state is attained in this case is ~3 μs (see figure 3). In this situation, the *j-U* characteristics represented by curves 1 and 2 in figure 4 can not be considered isothermal. Indeed, an estimate of ΔT by formula (1) at $j = 7200$ A cm^{-2}, $U = 22.5$ V, $t_0 = 3 \times 10^{-6}$ s (see curve 1 in figure 4) gives $\Delta T \approx 30$ K at $T = 297$ K. At $T = 460$ K, the estimate by (1) at $j = 4560$ A cm^{-2}, $U = 20$ V, (see curve 2 in figure 4), C (460 K) = 0.69 J gK^{-1}, and χ(460 K) = 0.58 cm^2 s^{-1} [18] yields $\Delta T \approx 21$ K. Curves 1 and 2 can be used as 'isothermal' *j-U* characteristics for electro-thermal calculations only for very rough estimates.

If the base of the device is modulated by minority carriers, these carriers are to be removed from the base when the reverse bias is applied. This diminishes the operating speed of the device. At the same time, it was mentioned above that the base modulation reduces the voltage drop across the device and, consequently, makes ΔT lower.

If there is no base modulation (curves 1″ and 2″ in figure 4). the estimate of ΔT in accordance with formula (1) at $t_0 = 3 \times 10^{-6}$ s gives $\Delta T \approx 48$ K ($j = 6720$ A cm^{-2}, $U = 38$ V) at 297 K and $\Delta T \sim 31$ K ($j = 3600$ A cm^{-2}, $U = 38$ V) at 460 K.

It can be seen in figure 3 that the characteristic time in which the steady-state is attained when there is hole injection is determined by hole lifetime in the base of the structure. This means that the *isothermal* current–voltage characteristics in structures of this kind cannot, *in principle*, be measured experimentally [24]. The same situation occurs in high-voltage silicon carbide and gallium nitride rectifiers. In these cases, isothermal current–voltage characteristics should be 'reconstructed' from experimental pulsed current–voltage curves by comparison with an adequate analytical or numerical model [24]. However, in contrast to high-voltage rectifier diodes, there is no adequate theory for JBS.

4. Conclusion

Isothermal forward current–voltage characteristics were measured in 4H-SiC JBS with a blocking voltage of 1700 V up to a current density $j \approx 4200$ A cm^{-2} in the temperature range 297–460 K. The pulsed forward *j-U* characteristics were measured 120 ns after the bias pulse was applied. The overheating ΔT at $j = 4200$ A cm^{-2} ($U = 22.5$ V, $t_0 = 1.2 \times 10^{-7}$ s) was $\Delta T \approx 2$ K at 297 K and monotonically decreased with increasing temperature. If there is hole injection, the voltage drop across the device approaches the steady-state condition $t \leq 3\,\mu$s after the pulsed bias is applied. The time in which the steady-state is attained in this case is apparently determined by hole lifetime in the base of the structure. In the mode with hole injection, $\Delta T \approx 30$ K at $j = 7200$ A cm^{-2}, ($U = 22.5$ V, $t_0 = 3 \times 10^{-6}$ s) at 297 K and $\Delta T \approx 21$ K at $j = 4560$ A cm^{-2}, ($U = 20$ V) at 460 K.

Acknowledgments

This work was partly supported at the Ioffe Physical—Technical Institute by Cree Inc. and the Russian Foundation for Basic Research.

References

[1] Kimoto T and Cooper J 2014 *Fundamentals of Silicon Carbide Technology: Growth, Characterization, Devices and Applications* (New York: Wiley)
[2] Hillkirk L M 2004 *Solid State Electron.* **48** 2181

[3] Levinshtein M E, Mnatsakanov T T, Ivanov P A, Palmour J W, Das M K and Hull B A 2008 *Semicond. Sci. Technol.* **23** 085011
[4] Levinshtein M E, Ivanov P A, Mnatsakanov T T, Palmour J W, Das M K and Hull B A 2008 *Solid-State Electron.* **52** 1802
[5] Baliga J 1987 *IEEE Electron Devices Lett.* **8** 407
[6] Singh R, Capell C D, Hefner A R, Lai J and Palmour J W 2002 *IEEE Trans. Electron Devices* **49** 2054
[7] Wu J, Fursin L, Li Y, Alexandrov P, Weiner M, and Zhao J H 2006 *Semicond. Sci. Technol.* **21** 987
[8] Perez-Tomas A, Brosselard P, Hassan J, Jorda X, Godignon P, Placidi M, Constant A, Millan J and Bergman J P 2008 *Semicond. Sci. Technol.* **23** 125004
[9] Caldwell J D, Stahlbush R E, Imhoff E A, Hobart K D, Tadjer M J, Zhang Q and Agarwal A 2009 *J. Appl. Phys.* **106** 044504
[10] Buttay C, Raynaud C, Morel H, Civrac G, Locatelli M-L and Morel F 2012 *IEEE Trans. Electron Devices* **59** 761
[11] Levinshtein M, Mnatsakanov T, Ivanov P, Palmour J, Das M and Hull B 2007 *Solid-State Electron.* **51** 955
[12] Carslow H and Jager J 1959 *Conduction of Heat in Solids* (Oxford: Clarendon)
[13] Maas B L, Clements N D and Rinaldi V 1993 *IEEE Trans. Magn.* **29** 1017
[14] Johnson C M, Rahimo M, Wright N G, Hinchley D A, Horsfall A B, Morrison D J and Knights A 2000 *Industry Applications Conf. 2000. Conf. Record of the 2000 IEEE* vol 5, p 2941
[15] Perez R, Mestres N, Vellveh M, Godignon P and Mill J 2006 *Semicond. Sci. Technol.* **21** 670
[16] Cappelluti F, Bonani F and Ghione G 2009 *Proc. of the Int. Semiconductor Device Research Symp.* (*College Park, MD, USA, December 9–11 2009*) pp 1–2
[17] Cree 2010 *CPW3-1700S010 Silicon Carbide Schottky Diode Chip* www.cree.com/~/media/Files/Cree/Power/Data%20 Sheets/CPW31700S010B.pdf
[18] Levinshtein M E, Rumyantsev S L and Shur M S (ed) 2001 *Properties of Advanced Semiconductor Materials: GaN, AIN, InN, BN, SiC, SiGe* (New York: Wiley)
[19] Shaffer W, Kong H S, Negley G H and Palmour J W 1994 *Proc. of the 5th Conf. on Silicon Carbide and Related Materials, Institute of Physics Conf. Series* vol 137, p 155
[20] Khan I A and Cooper J A Jr 2000 *IEEE Trans. Electron Devices* **47** 269
[21] Shockley W 1961 *Solid State Electron.* **2** 35
[22] Kressel H 1967 *RCA Rev.* **28** 175
[23] Gonzalez J R, Rey-Stolle I, Algora C and Galliana B 2005 *IEEE Electron Devices Lett.* **26** 867
[24] Levinshtein M E, Mnatsakanov T T, Ivanov P A, Palmour J W, Das M K and Hull B A 2007 *Semicond. Sci. Technol.* **22** 253